Talanta 81 (2010) 404–411

Contents lists available at ScienceDirect

Talanta

journal homepage: www.elsevier.com/locate/talanta

Sequential identification of organic dyes using the voltammetry of microparticles approach

Antonio Doménech-Carbó [a,*], María Teresa Doménech-Carbó [b], Marina Calisti [a], Vincenzo Maiolo [a]

[a] Departament de Química Analítica, Universitat de València, Dr. Moliner, 50, 46100 Burjassot (València), Spain
[b] Institut de Restauració del Patrimoni, Universitat Politécnica de València, Camí de Vera 14, 46022, València, Spain

ARTICLE INFO

Article history:
Received 28 October 2009
Received in revised form 4 December 2009
Accepted 10 December 2009
Available online 16 December 2009

Keywords:
Voltammetry of microparticles
Organic dyes
Polarization steps
Conservation and restoration
AFM
ATR-FTIR

ABSTRACT

An electrochemical method for identifying indigoid, anthraquinonic, naphtoquinonic, flavonoid, pyrone, pyran, and other related dyes in microsamples from works of art is reported using the voltammetry of microparticles methodology. Products of solid state oxidation/reduction of dyes form a layer on the lateral faces of the dye crystals as suggested by ATR-FTIR and AFM data. This method is based on the sequential application of oxidative and reductive constant-potential polarization steps coupled with the record of square wave voltammograms to solid microsamples of dyes in contact with aqueous electrolytes.

1. Introduction

The identification of organic dyeing components in works of art and archaeological materials is an obvious target for archaeometry, conservation and restoration [1,2]. Apart from the need to use minimal amounts of sample as possible (at the microgram level or less), analytical methods are conditioned by the high dilution of the colouring components in the matrix, and the simultaneous presence of minerals, binders, alteration products and other materials. Recently reported analytical methods for studying dyes in historical paints involve, among others [3], high performance liquid chromatography (HPLC) [4–9], gas chromatography [10,11] and infrared and Raman spectroscopies [12,13].

Along the last two decades, electrochemical methods have been applied for analyzing dyes in solution phase having different chromophores, including anthraquinone [14,15], azo [16–18] and reactive dyes [19,20]. Additionally, dye electrochemistry has received attention in relation with 'green chemistry' vat dyeing [21,22], their use as mediators for the indirect cathodic reduction of dispersed organic compounds [23–25] and mediators for electrocatalysis [26] and photoelectrocatalysis [27].

In this context, solid state electrochemical methods for analyzing dyes in work of art samples have been proposed [3,28,29]. These procedures are based on the voltammetry of microparticles (VMP), a methodology tailored by Scholz et al. [30–32], which provides highly sensitive electrochemical responses of solid materials with minimal amounts of sample, thus enabling for the characterization of organic solids [33–37]. The VMP methodology has been previously applied to the identification of anthraquinonic and naphtoquinonic [38,39], flavonoid [39,40], curcumoid [41] and indigoid [35,39,42] dyes in work of art and ancient textile samples, as well as indigo characterization in samples of Maya Blue pigment [43–46].

The electrochemical identification of individual dyes in real samples from works of art and archaeological pieces is made difficult, apart from the aforementioned general factors, by the similarity in the voltammetric responses of several dyes, frequently having close structural properties. In this report we present an electrochemical procedure for dye identification in solid microsamples using the VMP consisting on the sequential record of the square wave voltammetric responses of solid samples in contact with an aqueous electrolyte before and after the application of oxidative and reductive polarization steps. The proposed procedure is devoted to improve the diagnostic criteria for electrochemically identifying the most frequently used anthraquinone, naphtoquinone, indigoid, flavonoid, pyrone, pyran, and other related dyes, providing a sequential diagnostic criteria for discerning each one of those families of dyes and further distinguishing individual dyes within each group. This procedure, that extends those previously reported [38,40,41] and, in particular, that for discerning

* Corresponding author. Tel.: +34 963544533; fax: +34 963544436.
E-mail address: antonio.domenech@uv.es (A. Doménech-Carbó).

0039-9140/$ – see front matter © 2009 Elsevier B.V. All rights reserved.
doi:10.1016/j.talanta.2009.12.016

anthraquinonic dyes [28], is devoted to establish sequential diagnostic criteria for electrochemically discerning each one of those families of dyes and further distinguishing individual dyes within each group.

The studied dyes include: (a) anthraquinonic and naphtoquinonic dyes—alizarin (1,2-dihydroxy-9,10-anthraquinone), purpurin (1,2,4-trihydroxy-9,10-anthraquinone), and natural dyes aloe, cochineal red, madder, kermes, shellac and henna. Aloe is actually a mixture of aloin (aloin A: (10S)-10-glucopyranosyl-1,8-dihydroxy-3-(hydroxymethyl)-9(10H)-anthracenone, aloin B: (10R)-10-glucopyranosyl-1,8-dihydroxy-3-(hydroxymethyl)-9(10H)-anthracenone) and emodin (6-methyl-1,3,8-trihydroxyanthraquinone), while madder is a mixture of alizarin, purpurin, pseudopurpurin, alizarin 2-methyl ether, rubiadin and munjistin. Henna is composed of a mixture of two naphtoquinones, lawsone (2-hydroxy-1,4-naphthoquinone) and juglone (5-hydroxy-1,4-naphthoquinone). Shellac consists of a mixture of laccaic acids, whereas kermes and cochineal red are constituted, respectively, by kermesic acid and carminic acid, as colouring components. (b) Flavonoid, pyran and pyrone dyes, including luteolin, morin, dragoon's blood, weld, old fustic, gamboge, Brazilwood and logwood. Luteolin (3′,4′,5,7-tetrahydroxyflavone) is the main colouring component of weld (or *arizca*) while morin (2′,3,4′,5,7-pentahydroxyflavone) is the colouring agent of old fustic, with maclurin and moritamnic acid as minor components. The main component of gamboge is gambogic acid, whereas dracorubin and draco-hordin are the pigmenting agents of dragoon's blood. In turn, Brazilwood is composed of a mixture of brazilin ((6a*S*,11b*R*)-7,11b-dihydro-6*H*-indeno[2,1-*c*]chromene-3,6a,9,10-tetrol) and brazilein (6a,7-dihydro-3,6a,10-trihydroxy-benz[b]indeno[1,2-d]pyran-9(6H)-one), compounds of similar structure to those of hematein (3,4,6a,10-tetrahydroxy-6,7-dihydroindeno[2,1-c]chromen-9-one) and hematoxylin (7,11b-dihydroindeno[2,1-c]chromene-3,4,6a,9,10(6H)-pentol), responsible of the coloration of logwood (or litmus Campeche). (c) The main curcumoid dyes are safflower, obtained from *Carthamus tinctoria* and composed of a mixture of carthomone, carthamin and pricarthamin, and curcuma, obtained from *Curcuma longa*, whose main colouring component is curcumin (1,7-bis(4-hydroxy-3-methoxyphenyl)-1,6-heptadiene-3,5-dione. (d) Indigotin (3H-indol-3-one, 2-(1,3-dihydro-3-oxo-2H-indol-2-ylidene)-1,2-dihydro) is the colouring agent of indigo dye, extracted from different plants, namely, *Indigofera tinctoria* (India), *Indigofera indigotica* (or *tein-cheing*, *China*), *Polygonum tinctorium* (the Far East), *Isatis tinctoria* (Europe) and *Indigofera suffruticosa* (Mesoamerica). Tyrian purple is its 6,6′-dibromo derivative, obtained from several muricides such as *Murex brandaris*, such dyes being the most representative of the indigoid group.

Within the studied systems, we include saffron and sepia. Although the hue of saffron (extracted from *Crocus sativus*) is mainly due to the degraded carotenoids (crocin and crocetin), the flavor comes from the carotenoid oxidation products, mainly safranal, (2,6,6-trimethylcyclohexa-1,3-dien-1-carboxaldehyde), 2,2,6-trimethyl-1,4-cyclohexanedione, 4-ketoisophorone and 2-hydroxy-4,4,6-trimethyl-2,5-cyclohexadien-1-one [47]. In turn, sepia is a dark-blue pigment obtained from *Seppia officinalis*, constituted of melanin polymers mainly derived from eumelanin and eomelanin.

In the present study, cyclic and square wave voltammetries, controlled potential coulometry and chronoamperometry have been applied in parallel to atomic force microscopy (AFM) and attenuated total reflectance-Fourier transform infrared spectroscopy (ATR-FTIR) in order to characterize possible mechanisms involved in electrochemical processes, in correlation with the theoretical model developed by Lovric, Scholz, Oldham and coworkers [48–52]

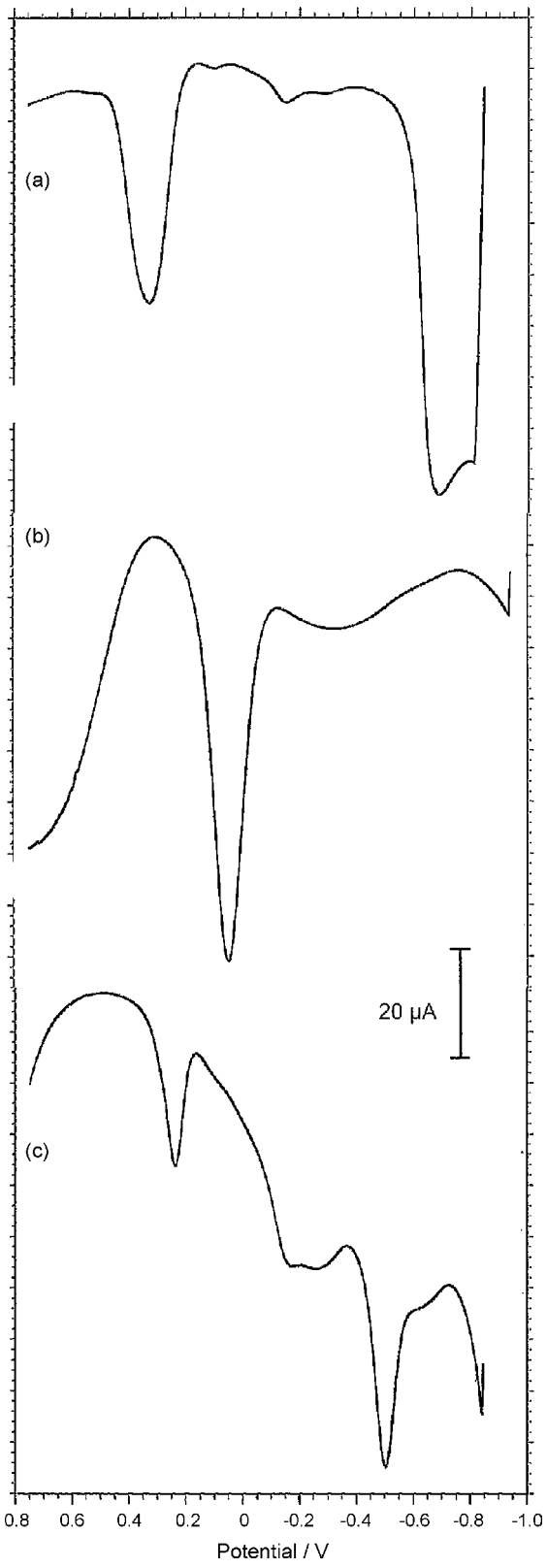

Fig. 1. SWVs for (a) morin-, (b) alizarin- and (c) indigo-modified PIGEs immersed into 0.50 M potassium phosphate buffer (pH 7.0). Potential initiated a −0.85 V in the positive direction. Potential step increment 4 mV; square wave amplitude 25 mV; frequency 5 Hz.

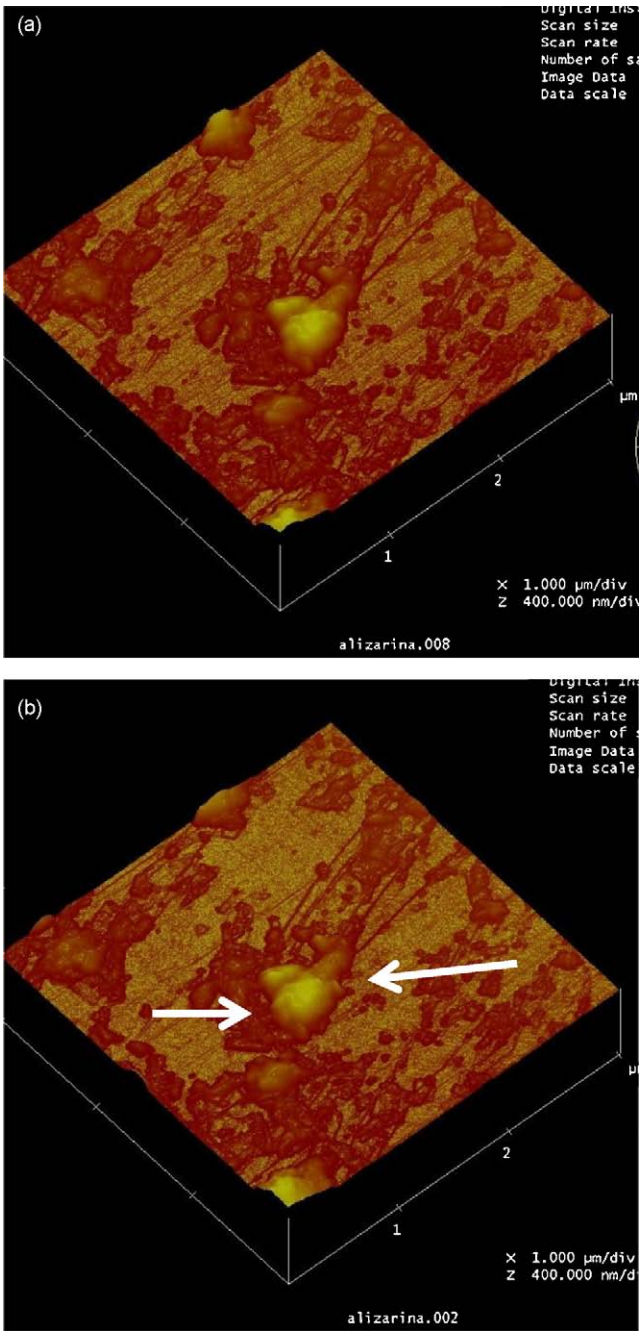

Fig. 2. Topographic AFM images of morin crystals adhered to a graphite plate in contact with 0.50 M aqueous sodium acetate buffer before (a), and after (b) application of a linear potential scan between 0.00 and +1.0 V at a sweep rate of 10 mV/s.

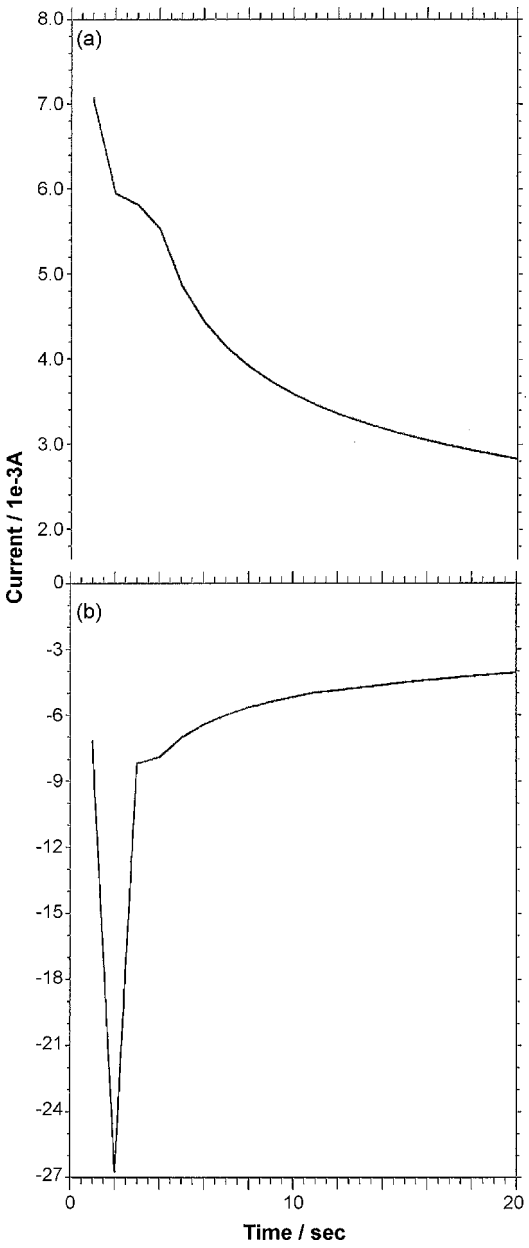

Fig. 3. Chronoamperometric curves for indigo microparticles attached to PIGE in contact with 0.50 M sodium acetate buffer (pH 4.75) under applied potentials of: (a) −0.35 V, (b) +0.50 V.

thus extending prior results on the electrochemistry of organic dyes [53,54]. Square wave voltammetry (SWV) has been used as a detecting technique by its high sensitivity and immunity to capacitive effects. This technique, whose theory for immobilized reactants was developed by Lovric, Komorsky-Lovric and Bond [55,56], is of interest with regard the electrochemistry of solids [57].

2. Experimental

Alizarin, purpurin, luteolin and morin (Sigma) and indigo (Fluka) reagents were used as reference materials. Carmine (cochineal type from *Coccus cacti* insect), curcuma, safflower, dragoon's blood, and gamboge were supplied from AP Fitzpatrick. Shellac from *Coccus lacca* (K 36020), red henna (K 37500) aloe (K 38010), madder (K 37202), weld (K 37202), Brazilwood (K 36150), logwood (K 36100), Tyrian purple (K 36010) and saffron (K 37110) were Kremer pigments. An aqueous 0.50 M potassium phosphate solution (Buffer, pH 7.0) (Panreac) was used as a supporting electrolyte.

Paraffin-impregnated graphite electrodes (PIGEs) consist on cylindrical rods of 5 mm diameter of graphite impregnated under vacuum by paraffin [18–20]. To prepare dye-modified PIGEs, 0.1–1 mg of the material was powdered in an agate mortar and pestle, and placed on a glazed porcelain tile forming a spot of finely distributed material and then abrasively transferred to the surface of a PIGE by rubbing the electrode over that spot of sample.

Electrochemical experiments were performed at 298 K in a three-electrode cell under argon atmosphere using a Ag/AgCl/3 M NaCl reference electrode (BAS MF 2010) and a platinum-wire auxiliary electrode. Cyclic and square wave voltammograms (CVs and SWVs, respectively) were obtained with a CH 420I equipment.

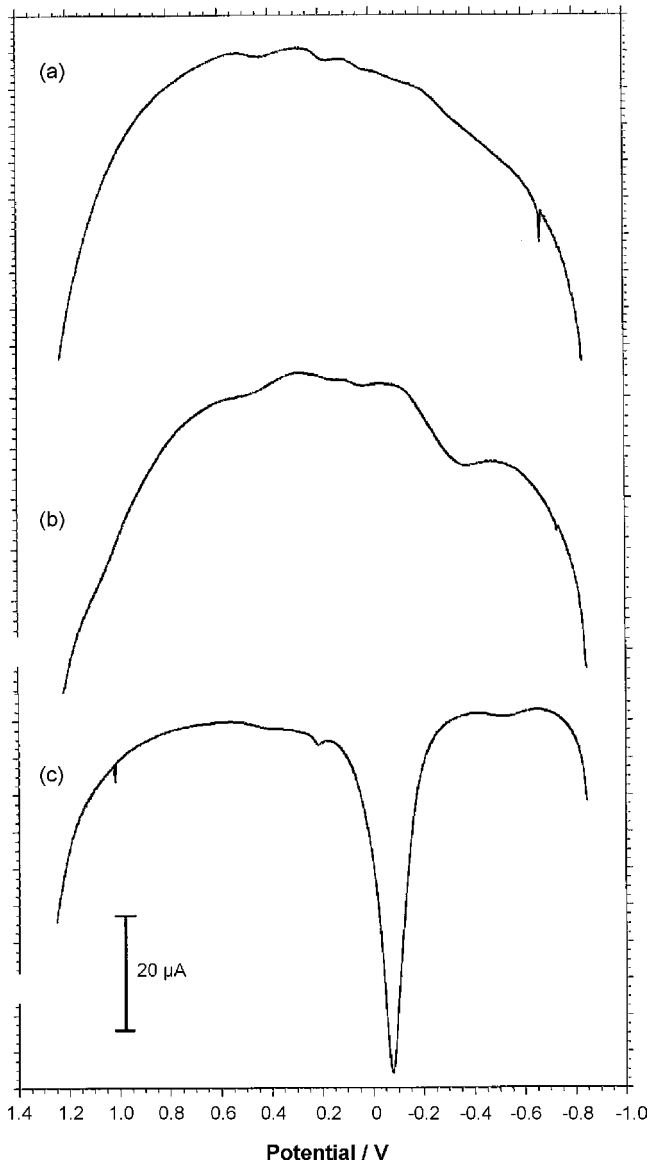

Fig. 4. SWVs for sepia microparticles attached to PIGEs in contact with 0.50 M potassium phosphate buffer (pH 7.0). (a) pristine sepia deposit, and (b and c) sepia deposits after application during 10 min of a potential step: (b) at +1.25 V; (c) at −1.25 V. Potential initiated at −0.75 V in the positive direction. Potential step increment 4 mV; square wave amplitude 25 mV; frequency 5 Hz.

SQWVs at dye-modified PIGEs were performed on initiating the potential scan either at +1.25 and −0.85 V using a potential step increment of 4 mV and a square wave amplitude of 25 mV. The frequency was varied from 2 to 200 Hz. LSVs and CVs were performed at potential scan rates ranging between 20 and 500 mV/s. Polarization steps were performed by applying potentials between −1.50 or +1.50 V during times between 2 and 15 min to freshly modified electrodes. After this polarization step, detection scans are performed using the conditions described in the above paragraph.

ATR-FTIR spectra were obtained with a Perkin Elmer BX Spectrum Fourier transform infrared spectrometer. Number of co-added scans: 24; resolution: 4 cm^{-1}. Spectra were obtained at fluorine-doped tin oxide electrodes (FTOs, Flexitec) covered by microparticulate deposits of alizarin and indigo, dried in air, before and after applying different potential steps in contact with phosphate buffer.

A Multimode AFM (Digital Instruments VEECO Methodology Group) with a NanoScope IIIa controller and equipped with a J-type

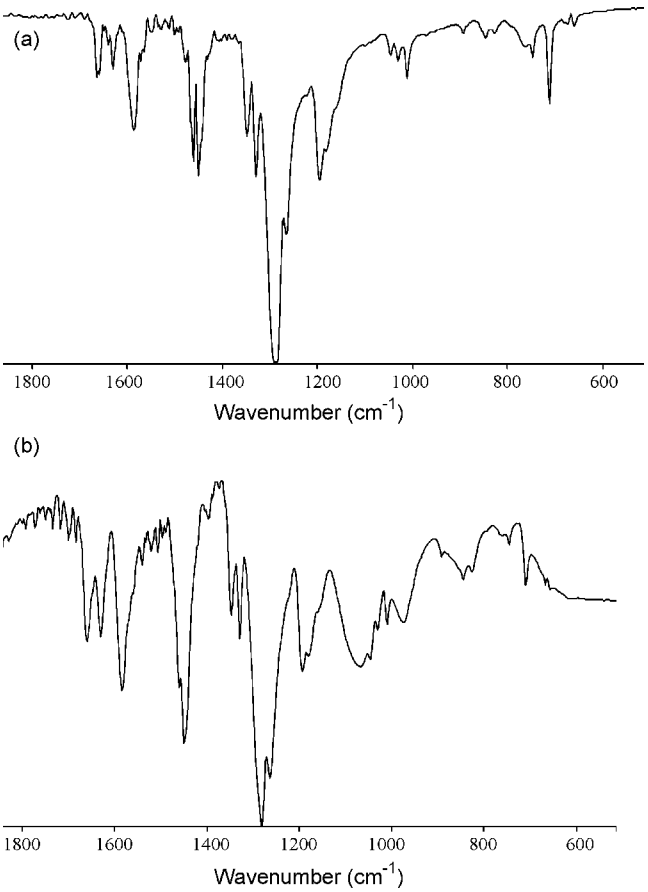

Fig. 5. ATR-FTIR spectra of alizarin-modified FTO electrodes, (a) before, and (b) after application of a constant potential step of +1.0 V during 30 min in contact with potassium phosphate buffer.

scanner (maximum scan size of 150 μm × 150 μm × 6 μm) was used. The topography of the samples was studied in contact mode. An oxide-sharpened silicon nitride probe Olympus, VEECO Methodology Group, model NP-S has been used with a V-shaped cantilever configuration. The spring constant is 0.06 N/m and the tip radius of curvature is 5–40 nm. For electrochemical measurements, the AFM was coupled to a Digital Instruments universal bipotentiostat (VEECO Methodology Group). All measurements were performed at room temperature in solutions previously deaerated by bubbling argon during 15 min. Statistical analyses were performed with the Minitab 14 software package.

3. Results and discussion

3.1. Electrochemical mechanisms

As described in literature [28–40], voltammetry of organic dyes in contact with aqueous media involve both oxidation and reduction proton-assisted solid-state electron transfer processes and, eventually, reductive or oxidative dissolution processes. Fig. 1 shows typical SWVs initiated at −0.75 V vs. Ag/AgCl/3 M NaCl in the positive direction for: (a) morin-, (b) alizarin- and (c) indigo-modified PIGEs immersed into phosphate buffer. Oxidation processes at +0.25 V for morin and +0.40 V for alizarin can be attributed to the oxidation of the o-diphenol moieties to the corresponding quinone [38–40]. The parent quinone group of alizarin is also reduced to the diphenol at −0.72 V. Indigo is oxidized to dehydroindigo at +0.35 V and reduced to leucoindigo at −0.40 V [35].

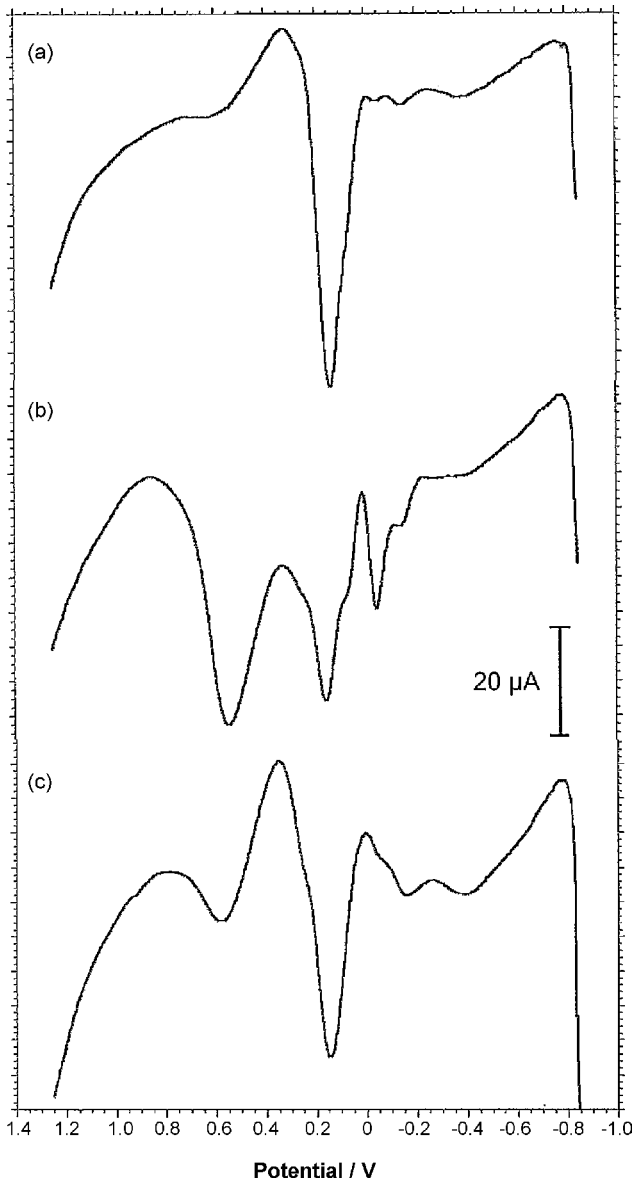

Fig. 6. SWVs for PIGEs modified with: (a) Brazil wood, (b) a 50:50 (w/w) Brazil wood plus logwood mixture, and (c) logwood, in contact with 0.50 M phosphate buffer (pH 7.0). Potential initiated at −0.85 V in the positive direction. Potential step increment 4 mV; square wave amplitude 25 mV; frequency 5 Hz.

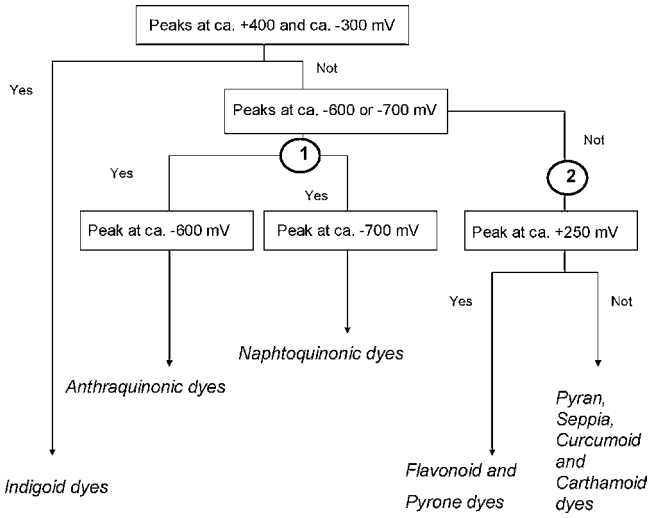

Fig. 7. Identification scheme using voltammetric data in Table 1 for discerning between the families of dyes studied here.

This voltammetry can be rationalized on the basis of the theoretical models developed by Lovric, Scholz, Oldham and coworkers [48–52]. For sparingly soluble organic compounds, the electrochemical process initiates at the particle/electrode/electrolyte interface and propagates through coupled proton and electron transfer processes over the surface and into the body of the particle. Charge transport occurs via proton hopping and electron hopping between adjacent molecules in the solid, charge conservation requiring the simultaneous ingress (or issue) of electron and protons in the solid particles in reduction (or oxidation) processes. Analysis of chronoamperometric data for different dyes using the aforementioned model indicated that proton hopping is slower than electron hopping in organic solids [53,54]. As a result, proton-assisted reduction and oxidation processes should be localized in a shallow layer in the vicinity of the particle/electrolyte interface, in agreement with expectances from the Lovric and Scholz model with significantly restricted proton diffusion across the solids.

As previously reported [38,40,41], under repetitive voltammetry, the electrochemical response becomes more complicated because additional oxidation and/or reduction peaks are recorded in the second and successive scans. The appearance of additional voltammetric peaks can be attributed to the electrochemical response of the new products formed during the initial oxidation or reduction of the parent product.

In situ atomic force microscopy (AFM) images of crystals of morin and indigo recorded along the electrochemical oxidation/reduction of such compounds in contact with aqueous acetate buffer are consistent with the above expectances. Fig. 2 shows in situ topographic AFM images from the upper face and sides of crystals of morin: (a) before, and, (b) after application of a linear potential step between 0.0 and +1.0 V. Here, an agglomerate of crystals of ca. 1 μm × 0.5 μm exhibits significant changes during the potential scan, consisting of an apparent erosion of several regions of lateral sides, while several minor crystals apparently growth (continuous arrow) with a maximum extent of ca. 50–80 nm. As judged by these morphological changes, the advance of the electrochemical reaction decays rapidly with time, thus denoting that no reductive/oxidative dissolution processes occur under our experimental conditions. Interestingly, the thickness of the lateral layer is essentially identical to the effective breadth of the electroactive layer calculated from the values for the diffusion coefficients of protons (D_H) and electrons (D_e) [53,54], which in turn, can be estimated from chronoamperometric data using the Lovric and Scholz model [48–52] (typical values in contact with potassium phosphate buffer are $D_H = 2 \times 10^{-10}$ cm^2/s and $D_e = 8 \times 10^{-7}$ cm^2/s).

As previously discussed [46,54], it appears that the solid state reduction or oxidation of dyes takes initially place without morphological disintegration as a topotactic process eventually accompanied by exfoliation and restacking, similarly to other processes [58,59]. At longer times, the advance of the electrochemical reaction through the crystals should involve a significant crystal re-structuring and eventually phase transition, as suggested by voltammetric curves at different timescales [46]. The appearance of phase transition steps is in principle consistent with long-time chronoamperometric data, as illustrated in Fig. 3. Here, current/time curves for (a) the reduction of indigo (applied potential −0.35 V), and, (b) its oxidation (applied potential +0.50 V), are shown. In both cases, the current initially decreases until a transient current growth at ca. 4 min appears, followed by

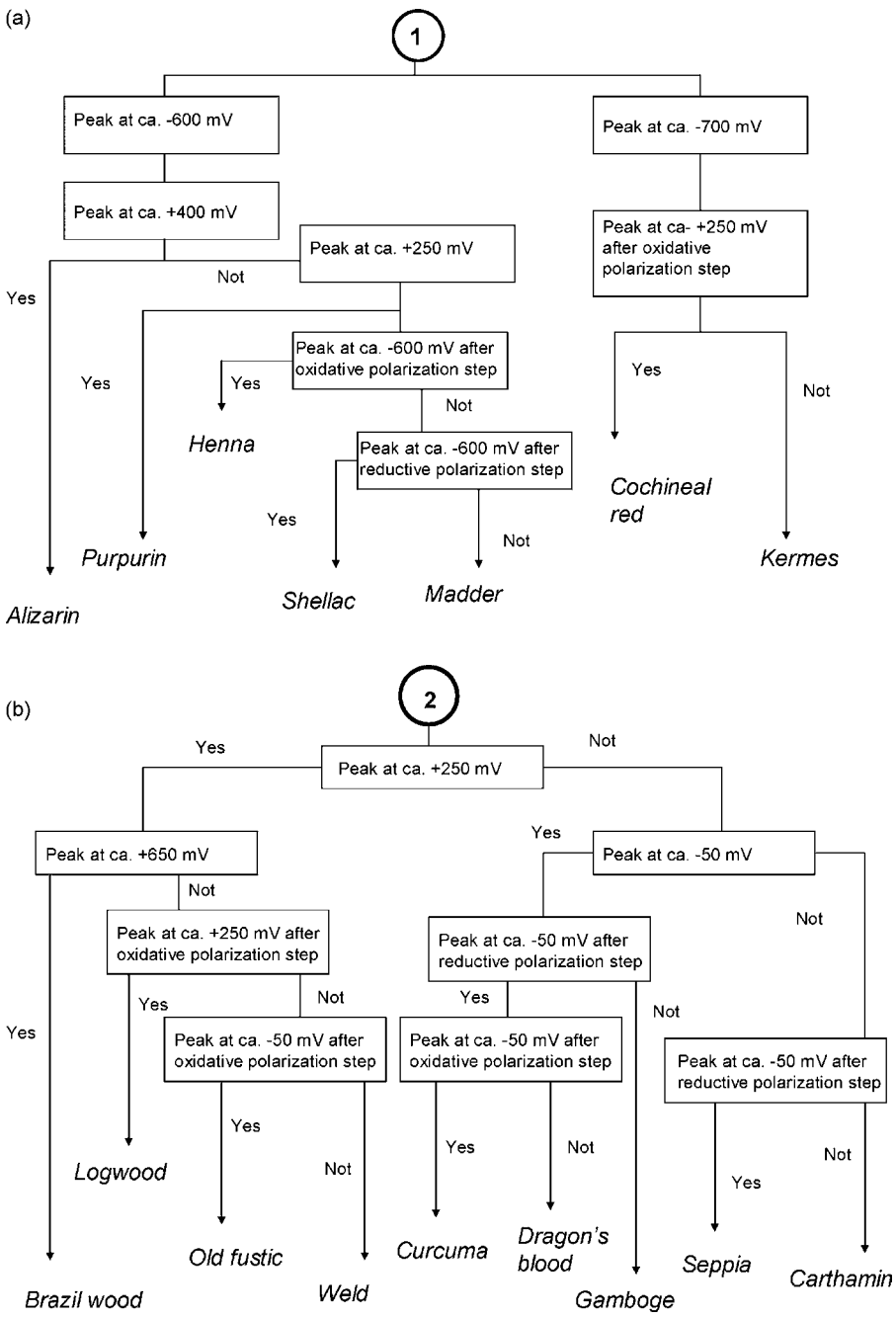

Fig. 8. Scheme for the identification of individual (a) anthraquinonic and naphtoquinonic, (b) flavonoid, pyran, curcumoid, carthamoid and sepia dyes studied here using voltammetric data in Table 1.

a monotonically decreasing current at longer times. This situation parallels that existing in, for instance, nucleation processes in the electrodeposition of quinolein derivatives on mercury electrodes [60,61] and layer-by-layer electrodeposition processes [62,63], thus suggesting that the formation of a new phase is involved.

The possibility of formation of new phases of oxidized or reduced products and the appearance of additional redox processes at separated potentials is consistent with the recognized structural flexibility of the majority of involved organic compounds. In fact, conformational changes in dye molecules can produce significant changes in terms of electronic properties as discussed for hematoxylin/haematein by Shirai and Matsuoka [64] and morin hydrate by Wu et al. [65].

3.2. Application of polarization steps

Although voltammetric responses for selected dyes are significantly different (see Fig. 1), discerning between dyes of the same family is often difficult [38–41]. The difficulty for identifying individual dyes is increased in real samples due to the frequent use of mixtures of dyes and the presence of interfering compounds. Accordingly, introduction of analytical strategies is of interest for discerning individual dyes. The application of a constant potential at relatively high negative or positive potentials should produce a layer of reduction or oxidation product(s) in a narrow surface region of the particles. Then, application of different potential stages can lead to the formation of different layers along the potential steps. This is consistent with the observations of Grygar et al. [39] and

Dai and Shin [66] relative to the high sensitivity of anthraquinone electrochemistry to the application of different polarization steps. The application of a subsequent potential scan should produce significant changes in the voltammetric response due to the presence of new product(s) [54], thus increasing the disposable diagnostic criteria for identifying the parent compound (*vide infra*).

Remarkably, in most cases, the voltammetric record changes significantly upon application of polarization potentials. In the case of sepia (Fig. 4), the pristine material remains electrochemically silent, as well as after application of oxidative potential steps. After reductive step, however, a prominent oxidation signal is recorded. The appearance of different voltammetric responses after application of reductive or oxidative potential steps can be attributed to the formation of layers of oxidable/reducible new crystalline phases whose electrochemical response differs from that of the parent compound.

Interestingly, the post-polarization voltammograms recorded at times longer than 5 min were essentially identical, thus suggesting, in agreement with a prior chronoamperometric data [54], that the redox reaction of dyes is rapidly exhausted. ATR-FTIR experiments confirm the formation of a layer of new compounds via electrochemical oxidation or reduction of dye microparticulate deposits. Thus, the oxidation and reduction of alizarin deposits on FTO electrodes results in the appearance of significant modifications in its infrared spectrum, as can be seen in Fig. 5. In particular, upon alizarin oxidation at +1.0 V, the morphology of 1258/1296 and 1452/1478 cm^{-1} bands, attributed, respectively, to (ν(CO)/ν(CC)/δ(CCC)) and ((ν(CC)/δ(COH)/δ(CCC)) vibrations [70,71], is clearly modified. New bands at 1395 cm^{-1} (ν(CC)/δ(CH)) and 1140 cm^{-1} (ν(CC)/δ(CH)/δ(CCC)) are recorded in the spectra obtained after electrochemical treatments.

Similarly, for indigo, intense bands at 1746 (ν(CO)/ν(CC)), 1677 (ν(CC)), 1592 (δ(CCring), δ(NH) and ν(CC)), 1559 (δ(CCring), δ(NH) and ν(CH)), and 1470 and 1451 cm^{-1} (δ(CCring), δ(NH) and δ(CH)) can be observed, in agreement with literature [67–69]. Upon electrochemical oxidation in contact with aqueous potassium phosphate buffer at +1.0 V during 30 min, the spectrum shows several significant changes: appearance of additional weak peaks in the 1800–1700 cm^{-1} region, around 1100 cm^{-1} and in the wavenumber range 1000–800 cm^{-1}. To rationalize these features, it can be taken into account that, following electrochemical data, only a narrow layer of oxidized product is formed in the lateral sides of indigo crystals. This implies that the contribution of the minority oxidized form to the resulting spectrum should be clearly lower than that of the parent indigo. Accordingly, differences can be more clearly seen just in the fingerprint 1000–800 cm^{-1} region where the bands of indigo are weaker. Remarkably, the band at 750 cm^{-1}, attributable to the γ(NH) mode, is considerably weakened upon oxidation, a feature which, in agreement with Tomkinson et al. [69] could characterize the pass from indigo to dehydroindigo.

3.3. Analytical performance

For our purposes, the relevant point to emphasize is that the application of oxidative and reductive polarization steps increases the number of parameters able to be used for identification with respect to the use of pristine material alone, thus increasing the analytical performance for the electrochemical recognition of the studied dyes. Obtained results for the studied dyes are summarized in Table 1. The use of a single set of peak potential data, however, makes difficult to discriminate individual dyes in dye mixtures. This can be seen in Fig. 6, where SWVs for (a) Brazil wood, (b) a 50:50 (w/w) Brazil wood plus logwood mixture, and (c) logwood, are shown.

Data in Table 1 are limited to the most intense voltammetric peaks because, in real samples from works of art, weak peaks can be significantly obscured by matrix effects. Repeatability test were performed for all dyes using 5 freshly prepared modified electrodes. In all cases, peak potentials exhibited standard deviations of 5–10 mV for pristine dyes and after application of oxidative or reductive potential steps during times of 5–10 min. Application of longer polarization steps results in larger dispersion of peak potential data. It should be noted that the increase in the number of available parameters enhances significantly the discerning ability of electrochemical data as can be seen on comparing cluster analysis. Examination of Table 1 reveals that, if data are limited to those obtained in the voltammograms of pristine dyes, distinction between several dyes cannot be obtained. Upon adding the complete set of data (including after polarization steps), all dyes can be separated and the percentage of difference in cluster analysis increases significantly.

Table 1
Peak potential data (mV vs. AgCl/Ag) recorded in the initial potential scan of freshly prepared dye-modified PIGEs (a) before, and, (b) after applying: (1) oxidative potential step of +1.50 V during 10 min, (2) a reductive potential step of −1.50 V during 10 min.

Dye	E_p (a)	E_p (b1)	E_p (b2)
Alizarin	+395* −600*	+383 −625 −715*	+605 −290 −715*
Henna	+250 −525	−620*	−620*
Shellac	−650*	+170	−590*
Purpurin	+295* −620	+285* +214* −650	+225 −215* −560*
Madder	+685 −300	+675 +365	+205 −715*
Cochineal red	+235 −720*	+235 −715	+205 −430
Kermes	+220 −695	+210	+190
Brazil wood	+650* +250*	+250*	+250*
Logwood	+250*		+250*
Gamboge	−50*		
Dragon's blood	−50*		−50*
Morin	+250*		
Old fustic	+250*		
Weld	−50*		+250*
Curcuma	−50*	−50*	−50*
Safflower			
Sepia			−50*
Saffron	−250 −700	−700	
Indigo	+240* −505*		+240* −505*
Tyrian purple	+230* −510*		+230* −510*
Isatin	+325* −680*		+325* −600*

Electrolyte: 0.50 M potassium phosphate buffer, pH 7.0. Potential scan initiated at −0.85 V in the positive direction. Potential step increment 4 mV; square wave amplitude 25 mV; frequency 15 Hz. The symbol * denotes particularly strong peaks.

For practical purposes, it is convenient to use identification sequences based, solely, in strong peaks in voltammograms recorded at dye-modified electrodes. Identification of saffron and safflower, both displaying weak peaks, remains uncertain. Fig. 7 shows an identification scheme for the groups of dyes studied here using SWVs initiated at −0.85 V in the positive direction. Combination of data for initial voltammograms and for voltammograms recorded after oxidative and reductive polarization steps provides a procedure for identifying each one of the dyes within each one of the above families. This is schematically depicted in Fig. 8, where identification schemes for individual (a) anthraquinonic and naphtoquinonic and (b) flavonoid, pyran, curcumoid, carthamoid and sepia dyes studied here using the voltammetric data listed in Table 1 is presented.

4. Conclusions

Solid organic dyes attached to graphite electrodes yield characteristic responses in contact with aqueous buffers. Application of constant potential polarization steps results in significant modifications of the voltammetric response. Solid state proton-assisted electrochemical processes result in the formation of narrow layers of oxidized/reduced products in the faces of the crystals of

involved organic compounds. These layers of oxidized or reduced compounds display characteristic voltammetric responses able to be used for identification purposes.

Dye identification can be obtained for discerning between the different types of pigments and for identifying the majority of the studied dyes using peak potential for the most intense voltammetric peaks before and after application of such polarization steps. This methodology enhances the number of parameters usable as diagnostic criteria for identifying dyes thus increasing the analytical performance of the voltammetry of microparticles in the field of conservation science.

Acknowledgements

Financial support is gratefully acknowledged from the Spanish I+D+I MICINN CTQ2008-06727-C03-01 and 02 Projects supported by ERDEF funds and the "Generalitat Valenciana" I+D+I GV04B/197 and ACOMP/2009/171projects. The authors would like to thank Mr. Manuel Planes i Insausti, technical supervisor responsible for the Electron Microscopy Service of the Universitat Politècnica de València.

References

[1] J.S. Mills, R. White, The Organic Chemistry of Museum Objects, 2nd. ed., Butterworth-Heinemann, London, 2001, pp. 121–133.
[2] E. Fitzhugh, A. Roy, R.L. Feller (Eds.), Artist's Pigments: a Handbook of their History and Characteristics, National Gallery of Art, London, 1997.
[3] A. Doménech, M.T. Doménech, V. Costa, Electrochemical Methods in Archeometry, Conservation and Restoration, Springer, Berlin, 2009.
[4] A. Quye, J. Wouters, J. Boon, Preprints of the 11th Triennial Meeting of ICOM Committee for Conservation, vol. 2, Edinburgh, 1996, pp. 704–713.
[5] J. Orska-Gawrys, I. Surowiec, J. Kehl, H. Rejniak, K. Urbaniak-Waleczak, M. Trojanowicz, J. Chromatogr. A 989 (2003) 239.
[6] B. Szostek, J. Orska-Gawrys, I. Surowiec, M. Trojanowicz, J. Chromatogr. A 112 (2003) 179.
[7] J. Sanyova, J. Reisse, J. Cult. Heritage 7 (2006) 229.
[8] J. Sanyova, Microchim. Acta 162 (2008) 361.
[9] I. Surowiec, W. Nowik, M. Trojanowicz, Microchim. Acta 162 (2008) 393.
[10] V. Sujata, G.A. Ravishankar, L.V. Venkataraman, J. Chromatogr. 624 (1992) 497.
[11] G.L. Alonso, M.R. Salinas, F.J. Esteban-Infantes, M.A. Sanchez Fernandes, J. Agric. Food Chem. 44 (1996) 185.
[12] H.G.M. Edwards, L.F.C. de Oliveira, A. Quye, Spectrochim. Acta A 57 (2001) 2831.
[13] L.F.C. de Oliveira, H.G.M. Edwards, E.S. Velozo, M. Nesbitt, Vibrat. Spectrosc. 28 (2002) 243.
[14] J. Zima, J. Barek, J.C. Moreira, V. Mejstrik, A.G. Fogg, Crit. Rev. Anal. Chem. 29 (1999) 125.
[15] J. Zima, J. Barek, J.C. Moreira, V. Mejstrik, A.G. Fogg, Fresenius J. Anal. Chem. 369 (2001) 567.
[16] J. Barek, H.P. Thuan, V. Mejstrik, J.C. Moreira, J. Zima, Anal. Lett. 31 (1998) 1219.
[17] J. Barek, H.P. Thuan, V. Mejstrik, J.C. Moreira, J. Zima, Collect. Czech. Chem. Commun. 62 (1997) 597.
[18] S. Combeau, M. Chatelut, O. Vittori, Talanta 56 (2002) 115.
[19] A. Fogg, M.V.B. Zanoni, A.R.H.M. Yusoff, R. Ahmad, J. Barek, J. Zima, Anal. Chim. Acta 362 (1998) 235.
[20] J. Barek, A.G. Fogg, J.C. Moreira, M.V.B. Zanoni, J. Zima, Anal. Chim. Acta 320 (1996) 31.
[21] R.S. Blackburn, A. Harvey, Environ. Sci. Technol. 38 (2004) 4034.
[22] M. Bozic, V. Kokol, Dyes Pigments 76 (2008) 299.
[23] T. Bechtold, E. Burtscher, D. Gmeiner, O. Bobleter, J. Electroanal. Chem. 306 (1991) 169.
[24] T. Bechtold, E. Burtscher, A. Turcanu, J. Electroanal. Chem. 465 (1999) 80.
[25] A. Vuorema, P. John, M. Keskitalo, M.A. Kulandainathan, F. Marken, Dyes Pigments 76 (2008) 542.
[26] H.R. Zare, N. Nasirizadeh, M. Mazloum-Arkadani, M. Namazian, Sens. Actuators B 120 (2006) 288.
[27] A. Hagfeldt, M. Grätzel, Chem. Rev. 95 (1995) 49.
[28] A. Doménech, M.T. Doménech, M. Calisti, V. Maiolo, J. Solid State Electrochem., in press. doi:10.1007/s10008-009-0898-x.
[29] A. Doménech, J. Solid State Electrochem., in press. doi:10.1007/s10008-009-0858-6.
[30] F. Scholz, B. Meyer, in: A.J. Bard, I. Rubinstein (Eds.), Electroanalytical Chemistry, A Series of Advances, 20, Marcel Dekker, New York, 1989, pp. 1–87.
[31] T. Grygar, F. Marken, U. Schröder, F. Scholz, Collect. Czech. Chem. Commun. 67 (2002) 163.
[32] F. Scholz, U. Schröder, R. Gulaboski, Electrochemistry of Immobilized Particles and Droplets, Springer, Berlin, 2005.
[33] F. Scholz, L. Nitschke, G. Henrion, Fresenius Z. Anal. Chem. 334 (1989) 56.
[34] A. Jaworski, Z. Stojek, F. Scholz, J. Electroanal. Chem. 354 (1993) 1.
[35] A.M. Bond, F. Marken, E. Hill, R.G. Compton, H. Hügel, J. Chem. Soc., Perkin Trans. 2 (1997) 1735.
[36] S. Komorsky-Lovric, V. Mircevski, F. Scholz, Mikrochim. Acta 132 (1999) 67.
[37] S. Komorsky-Lovric, J. Solid State Electrochem. 1 (1997) 94.
[38] A. Doménech, M.T. Doménech, M.C. Saurí, J.V. Gimeno, F. Bosch, Anal. Bioanal. Chem. 375 (2003) 1161.
[39] T. Grygar, S. Kucková, D. Hradil, D. Hradilová, J. Solid State Electrochem. 7 (2003) 706.
[40] A. Doménech, M.T. Doménech, M.C. Saurí, Talanta 66 (2005) 769.
[41] A. Doménech, M.T. Doménech, M.C. Saurí, Microchim. Acta 152 (2005) 75.
[42] A. Doménech, M.T. Doménech, M.L. Vázquez, J. Solid State Electrochem. 11 (2007) 1335.
[43] A. Doménech, M.T. Doménech, M.L. Vázquez, J. Phys. Chem. B 110 (2006) 6027.
[44] A. Doménech, M.T. Doménech, M.L. Vázquez, Anal. Chem. 79 (2007) 2812.
[45] A. Doménech, M.T. Doménech, M. Sánchez del Río, M.L. Vázquez, J. Solid State Electrochem. 13 (2009) 869.
[46] A. Doménech, M.T. Doménech, M.L. Vázquez, Archaeometry 51 (2009) 1015.
[47] L. Maggi, Luana, M. Carmona, P.C. del Campo, C.D. Kanakis, E. Anastasaki, P.A. Tarantilis, M.G. Polissiou, G.L. Alonso, J. Sci. Food Agric. 89 (2009) 1950.
[48] M. Lovric, F. Scholz, J. Solid State Electrochem. 1 (1997) 108.
[49] K.B. Oldham, J. Solid State Electrochem. 2 (1998) 367.
[50] M. Lovric, M. Hermes, F. Scholz, J. Solid State Electrochem. 2 (1998) 401.
[51] M. Lovric, F. Scholz, J. Solid State Electrochem. 3 (1999) 172.
[52] U. Schröder, K.B. Oldham, J.C. Myland, P.J. Mahon, F. Scholz, J. Solid State Electrochem. 4 (2000) 314.
[53] A. Doménech, M.T. Doménech, J. Solid State Electrochem. 10 (2006) 949.
[54] A. Doménech, M.T. Doménech, Electrochem. Commun. 10 (2008) 1238.
[55] S. Komorsky-Lovric, M. Lovric, A.M. Bond, Anal. Chim. Acta 258 (1992) 299.
[56] S. Komorsky-Lovric, J. Electroanal. Chem. 397 (1995) 211.
[57] M. Lovric, in: F. Scholz (Ed.), Electroanalytical Methods, Springer, Berlin, 2002, p. 111.
[58] U. Hasse, F. Scholz, Electrochem. Commun. 3 (2001) 429.
[59] Q. Feng, K. Kajiyoshi, K. Yanagisawa, Chem. Lett. 32 (2003) 48.
[60] C. Müller, J. Claret, F. Martínez, M. Sarret, J. Electroanal. Chem. 202 (1986) 203.
[61] C. Müller, J. Claret, M. Sarret, Electrochim. Acta 32 (1987) 283.
[62] S.K. Rangarajan, J. Electroanal. Chem. 46 (1973) 125.
[63] W. Obretenov, I. Petrov, I. Nachev, G. Staikov, J. Electroanal. Chem. 109 (1980) 195.
[64] K. Shirai, M. Matsuoka, Dyes Pigments 32 (1996) 159.
[65] T.-W. Wu, K.-P. Fung, L.-H. Zeng, J. Wu, A. Hempel, A.A. Grey, N. Camerman, Biochem. Pharm. 49 (1995) 537.
[66] H.-P. Dai, K.-K. Shin, Electrochim. Acta 43 (1998) 2709.
[67] M. Sánchez del Río, M. Picquart, M. Haro-Poniatowski, E. van Elslande, V.H. Uc, J. Raman Spectrosc. 37 (2006) 1053.
[68] M. Sánchez del Río, E. Boccaleri, M. Milanesio, G. Croce, W. van Beek, C. Tsiantos, G.D. Chyssikos, V. Gionis, G.H. Kacandes, M. Suárez, E. García-Romero, J. Mater. Sci. 44 (2009) 5524.
[69] J. Tomkinson, M. Bacci, M. Picollo, D. Colognesi, Vibrat. Spectrosc. 50 (2009) 268.
[70] M.V. Cañamares, J.V. García-Ramos, C. Domingo, S. Sánchez-Cortés, J. Raman Spectrosc. 35 (2004) 921.
[71] E.G. Kiel, P.M. Heertjes, J. Soc. Dyers Colour. 79 (2008) 21.